AIChE

R&D NOTES

A Novel Approach to Fabricate Macrovoid-Free and Highly Permeable PVDF Hollow Fiber Membranes for Membrane Distillation

Sina Bonyadi, Tai Shung Chung, and Raj Rajagopalan
Dept. of Chemical and Biomolecular Engineering, National University of Singapore, Singapore 117602

DOI 10.1002/aic.11688
Published online January 14, 2009 in Wiley InterScience (www.interscience.wiley.com).

Keywords: membrane distillation, hollow fiber, PVDF, membrane contactor, desalination

Introduction

The commercial polypropylene (PP) and Teflon (PTFE) hollow fiber membranes commonly applied for membrane distillation process are associated with drawbacks that limit the highest achievable flux through process. These fibers are normally fabricated by melt spinning and sintering that makes it difficult to fabricate membranes with high porosity (higher than 70%) and high degree of pores interconnectivity. Therefore, it is of great interest to fabricate alternative membrane contactors such as PVDF hollow fibers through phase inversion processes that provide more freedom to optimize membrane properties. Some progress has been made in fabrication of these fibers recently; however, optimizing membrane properties in accordance with some specific applications is yet to be investigated. Before we address the objectives of this article, we briefly review the essential characteristics of an ideal hollow fiber membrane applied in membrane distillation (MD).

High membrane permeability

Based on the MD mechanism,[1–4] highly gas permeable membranes are essential to achieve a high flux through the process. In this respect, membrane porosity has been known to be a key parameter influencing the membrane gas permeability.[1–4] As the membrane bulk porosity increases, the molecular and Knudson diffusivities of the vaporized molecules diffusing through the membrane increase in a proportional manner. Furthermore, as the membrane bulk porosity increases, the membrane thermal conductivity decreases and leads to a lower heat loss and a higher energy efficiency of the process.[2] It is also worthy to note that besides membrane bulk porosity, membrane surfaces must be highly porous as well, so that a high liquid–vapor interfacial area is formed at the membrane pore mouths.[1]

In addition to the membrane porosity, membrane morphology and pores interconnectivity are other determining factors that have been never discussed in the MD literature. However, there are a number of studies regarding the influence of these parameters in other membrane separation processes. Li and Chung[5] identified pore interconnectivity to have a great influence on the pure water permeability (PWP) of SPES hollow fibers applied in ultrafiltration. In other words, between two membranes with similar porosities, the membrane with an open cell structure or a high degree of pores interconnectivity will possess a higher permeability. In another study, Widjojo et al.[6] found that high pores interconnectivity in the supporting layer of the 6FDA-ODA-NDA/PSF dual-layer hollow fiber membranes could greatly reduce the substructure resistance in gas separation applications. Therefore, high porosity and high degree of pores interconnectivity should be maintained in order to maximize the membrane permeability.

High membrane wetting resistance and long-term stability

Membrane wetting is an undesirable phenomenon in MD that may lead to flux decay or lower separation efficiency.[1,2] Wetting usually occurs when the feed or permeate side pressure goes higher than the membrane critical liquid entry pres-

Correspondence concerning this article should be addressed to S. Chung at chencts@nus.edu.sg.

sure (LEP). LEP can be calculated through the following Laplace-Young equation[1,2]:

$$\Delta P = -\frac{2\gamma_L}{r}\cos\theta_{ef} \quad (1)$$

where ΔP is the pressure difference at the liquid-vapor interface, γ_L is the liquid-vapor surface tension, θ_{ef} is the effective contact angle, and r is the pore radius. To prevent the wetting phenomenon in long-term MD operations, membranes with high LEP, proper pore size distribution (0.1–0.5 μm)[2], and a reasonable degree of tortuosity are essential.

In term of membrane permeability, macrovoids may seem to form desirable membrane structures with low tortuosity and high porosity. But from a long-term performance point of view, macrovoids could be undesirable structures that enhance the wetting phenomenon in membranes, consequently reduce the membranes long-term stability. Therefore, fabrication of macrovoid-free and fully sponge-like membranes with sharp pore size distributions might enhance the membranes long-term stability.

Suitable membrane geometry and dimensions

Membrane wall thickness is a parameter that has a quite similar effect in all membrane applications. From a process productivity outlook, a thin wall is preferred to minimize the mass transfer resistance through the membrane, hence enhance the obtained flux from the process.[1] On the other hand, energy efficiency of the membranes requires that an optimized membrane thickness be adopted to suppress the heat loss through the membrane over energy consumed for water vaporization. Besides membrane thickness, another geometrical parameter comes into account in self-supported hollow fiber configurations, which is the fiber's inner diameter. Specially in a direct contact membrane distillation (DCMD) process, fibers with bigger inner diameters are usually preferred to allow for a higher permeate or feed flow rate through the fibers lumen side without exceeding the fibers LEP. Higher feed and permeate flow rates are desirable to prevent the excessive feed temperature drop or permeate temperature rise along the fibers, maintaining the temperature driving force across the membrane longitudinally.[1] However, from a mechanical stability point of view, the operating pressure and the mechanical properties of the membrane materials limit the smallest applicable wall thickness as well as the biggest inner diameter of the hollow fibers for each application. In this respect, the following dimensionless ratio (N) is normally used as a design parameter.

$$N = \text{fiber wall thickness}/\text{fiber ID} \quad (2)$$

As a rule of thumb for high pressure driven applications such as gas separations, $N = 0.5$ has been suggested by Ekiner et al.[7] However, in an MD process in which almost atmospheric pressures are applied, N values as low as $N = 0.1$ or less might be applicable as well. This translates into the applicability of a fiber with a small wall thickness as low as 100 μm at the same time, a big fiber ID as high as 1000 μm.

In summary, an ideal single layer MD fiber requires (1) a high porosity (>80%), (2) an optimum pore size and a sharp pore size distribution, (3) a macrovoid-free and open structure with interconnected pores, (4) a high water contact angle and a high LEP, (5) a small wall thickness (<150 μm) and a big inner diameter (1000 μm).

To the best of our knowledge, most of the fabricated PVDF fibers reported in the literature so far[8–12] are associated with a considerable number of macrovoids in the membrane matrix that might increase the wetting potential of the fibers in the long-term run. In our previous report,[1] we found that using weak coagulants such as 70–80 wt % methanol aqueous solution induces a delayed demixing in the PVDF dope solution that leads to a highly porous and open three-dimensional network with no macrovoids in the membrane structure. However, we observed that the nascent fiber formed during the delayed demixing process is rather weak mechanically to prevent the nascent fiber collapse or deformation during the spinning. In this communication, we intend to demonstrate a novel approach to overcome the obstacles in fabrication of single-layer PVDF hollow fibers with a small wall thickness and a big inner diameter ($N < 0.2$) with a similar highly permeable network-like morphology to our previously fabricated dual layer fibers. In other words, we aim to fabricate highly permeable macrovoid-free fibers with optimized dimensions to increase the maximum achievable flux in the MD process.

Experimental

Materials

PVDF HSV 900 was purchased from Arkema Inc. PAN was kindly supplied by Profs. J. Y. Lai and H. A. Tsai at Chung Yuan Christian University of Taiwan. *N*-Methyl Pyrrolidone (NMP) and methanol were used as solvent and nonsolvent, respectively, and supplied by Merck. Hydrophobic cloisite 15A particles were purchased from Southern Clay Products.

Dope preparation and fiber spinning

Table 1 shows the composition of the inner and outer layer dope solutions applied in the fiber spinning with other spinning conditions. More information regarding the properties of the clay particles incorporated in the two layers as well as the dope preparation approach can be found in Ref. 1. After dope preparation, the dual layer hollow fibers were fabricated through a dry-jet wet-spinning process using the spinning system described in detail elsewhere.[13]

Table 1. Spinning Conditions for the Dual Layer Hollow fibers

Outer layer dope concentration	PVDF HSV 900/hydrophobic clay particles/NMP (12.1 wt.%/3.6 wt.%/84.3 wt.%)
Inner layer dope concentration	PAN/NMP (15 wt.%/85 wt.%)
Bore fluid	Dl water/methanol (20 wt %/80 wt %)
Externa coagulant	Dl water/methanol (20 wt %/80 wt %)
Inner layer flow rate	1 ml/min
Outer layer flow rate	1.5 ml/min
Bore flow rate	1 ml/min
Length of air gap	3 cm
Take-up speed	Free fall
Post-treatment	Freeze drying

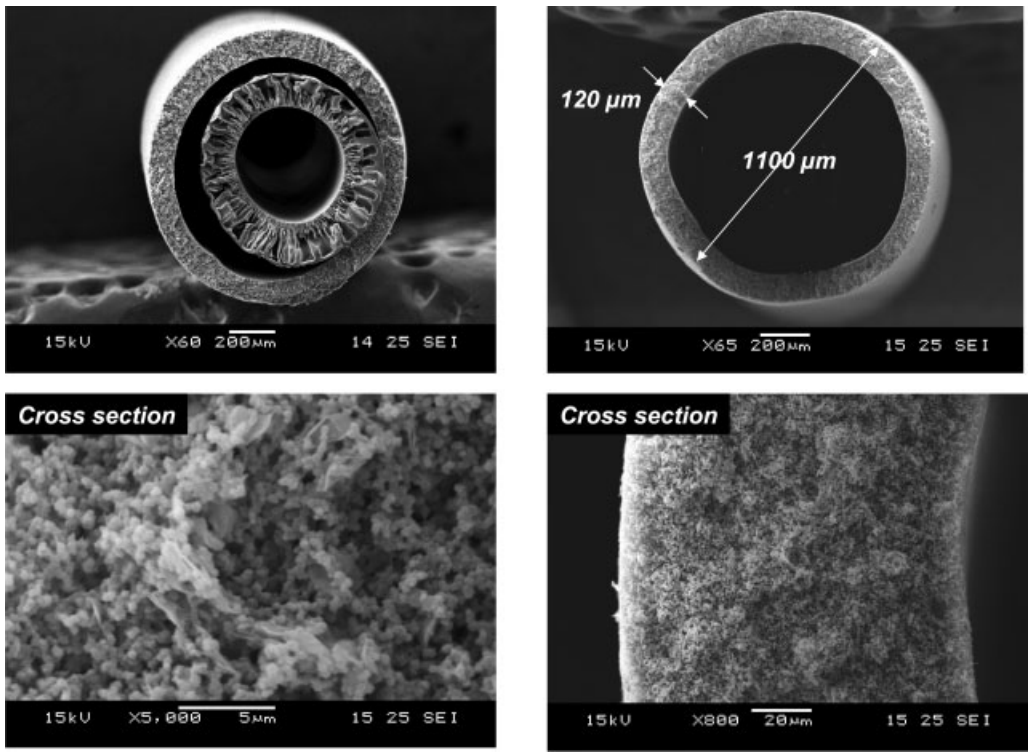

Figure 1. SEM micrographs showing the cross section morphology of the spun fibers in different magnifications.

Membrane characterization

For measuring the membranes contact angle, a Sigma 701 Tensiometer from KSV Instruments Limited was used. The sample hollow fibers were immersed into distilled water and the advancing contact angle was calculated with the aid of computer software. Ten readings were measured and an average was obtained from the results. All other characterizations such as Scanning Electron Microscopy (SEM), Gas permeation, Pore Size Distribution, and Porosity measurement were followed in the same ways as we reported previously.[1]

Direct contact membrane distillation experiments

Membrane modules were fabricated out of the spun fibers through a process, which is described in detail elsewhere.[14] Afterward, the modules were tested to desalinate 3.5 wt % brine feed water in a DCMD experimental set up in which feed stream went through the shell side of modules and permeate flowed through the fibers' lumen side. Further details about the experimental set up have been described in our previous report.[1] The ionic conductivity of the permeate stream was measured before and after the test using a Radiometer analytical conductivity meter (model Pionneer30) in order to calculate the separation factor.

Results and Discussion

Membrane characterization

The SEM micrographs in Figures 1 and 2 show the cross section and surface morphology of the fabricated fibers, respectively. As can be observed from these micrographs, the two layers of the fibers are totally delaminated mainly because of the different shrinkage percentage of the outer layer compared with the inner layer as well as the thermodynamically incompatible inner and outer dope solutions. The big difference in the shrinkage of the two layers is probably due to the stabilizing effect of the incorporated clay particles in the outer layer as well as the smaller precipitation rate of the outer layer as a result of the delayed demixing induced in the outer layer.[15] Furthermore, the thermodynamically different nature of outer layer (hydrophobic) and inner layer (hydrophilic) dope solutions might hinder the possible counter-diffusion of the two layers in the air-gap or coagulation regions.[15] From a morphological outlook, it can be observed that the outer functional layer has been formed in a desirable geometry with a small thickness (120 μm) and a big inner diameter (860 μm) without any deformation or collapse in the spinning line. In other words, it has a high concentricity with a uniform wall thickness. Furthermore, this layer is macrovoid-free and highly porous (porosity of 80%) with a sharp pore size distribution (average pore size of 0.44 μm), which all are in agreement with our previous observations.[1] The big delamination between the two layers allowed for the easy removal of the inner support layer even after mounting the fibers in the module. Therefore, the outer PVDF layer could be used as a single layer fiber in the MD process. Table 2 summarizes the characteristics of the functional PVDF layer.

Direct contact membrane distillation tests

The resultant single layer fibers were tested for the desalination of water in a DCMD process. The obtained flux as a function of the feed inlet temperature and other operating conditions has been tabulated in Table 3. It can be noticed

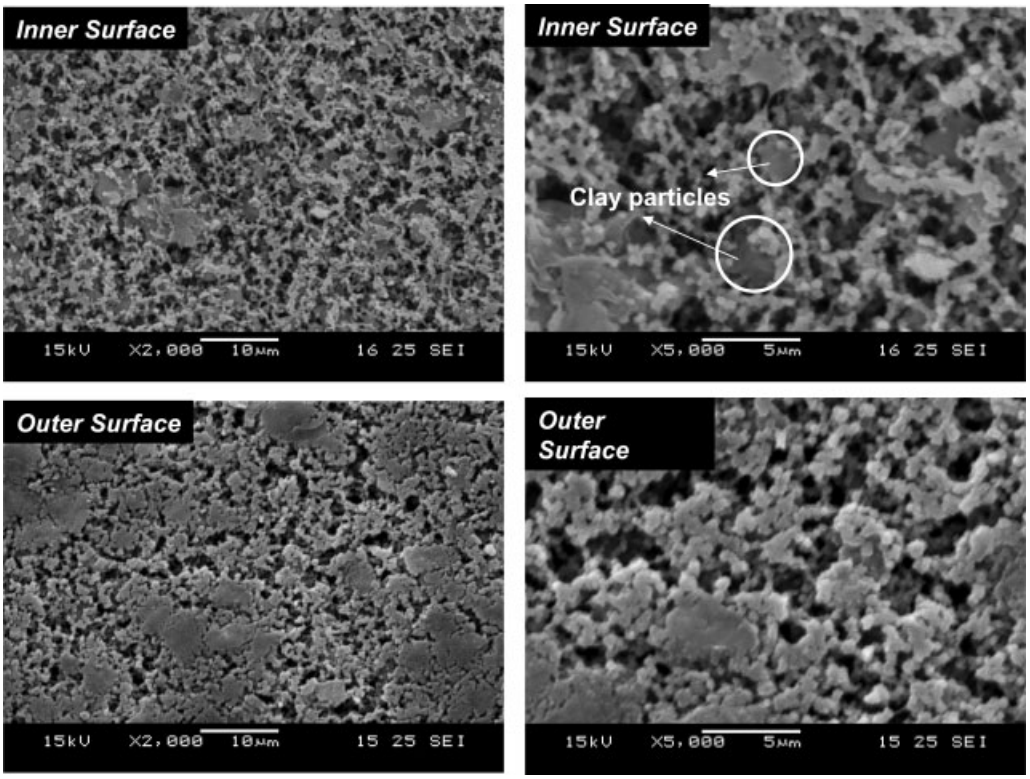

Figure 2. SEM micrographs showing the surface morphology of the functional PVDF layer.

that water vapor flux as high as 70 kg/m^{2}hr based on the fibers outer diameter has been achieved at 86 °C, which is considered as an outstanding flux in membrane distillation. This flux is even higher than the one obtained using the dual layer hydrophilic-hydrophobic fibers applied in our previous study.[1] This is probably due to the negative effect of the hydrophilic support layer in case of the dual layer fibers that introduces additional heat and mass transport resistances in to the permeate side of the fibers. Furthermore, a 100% salt rejection was obtained during the process. The initial ionic conductivity of the permeate stream was 14.02 μS/cm; whereas it decreased to 12.40 μS/cm at the end of the experiment. This might be resulted from the vaporization and condensation of highly pure water in the permeate side that had led to a less ionic conductivity of the permeate ultimately.

Figure 3 demonstrates the flux and the energy efficiency obtained in the DCMD process including some other flux data reported by the previous DCMD investigations using hollow fibers.[16–21] The energy efficiency in this study has been defined as the fraction of feed brine thermal energy that has been used to evaporate water. Energy efficiency can be easily calculated using the following equation:

$$\text{Energy Efficiency} = \frac{J\,\Delta H_v\,A_o}{\dot{m}_p\,C_p\,\Delta T_p}$$

where J is the water vapor flux, ΔH_v is water vapor latent heat of condensation, A_o is the total membrane area based on the fibers outer diameter, $\dot{m}_p$ is the permeate mass flow rate, C_p is the specific heat capacity of the permeate stream, and ΔT_p is the difference between permeate inlet and outlet temperatures. It can be observed that the obtained MD flux data in this study is comparatively higher than the previously reported data in the literature without carrying out any module design optimizations. The high obtained flux in this study confirms the importance of suitable membrane fabrication and engineering on the MD overall performance. Furthermore, it can be inferred from this figure that the energy efficiency of the process increases as a function of feed inlet temperature. The increases of energy efficiency as a function of feed inlet temperature is probably due to the fact that the driving force for water vaporization, i.e., water vapor partial pressure and consecutively energy consumption rate for water vaporization increase almost exponentially as a function of the operating temperature; whereas the energy lost by conduction through the membrane matrix increases linearly as a function of operating temperature.

Conclusions

The following conclusions can be drawn from this study: (1) dual layer spinning is an efficient approach to prevent

Table 2. Summary of Different Membrane Characteristics

Fiber wall thickness (μm)	120
Fiber OD (μm)	1100
N_2 Permeance cm^3 (STP)/(cm^2 s cmHg)	1.27
Porosity (ε)	80%
Average pore size (μm)	0.44
LEP (psig)	17

Table 3. DCMD Operating Conditions and the Obtained Flux for the Fabricated Fibers

Feed inlet temperature (°C)	50.1	60.9	72.2	79.9	86
Feed outlet temperature (°C)	49.5	59.9	70.5	78.3	83.8
Permeate inlet temperature (°C)	18	18.5	19.5	19.4	20.5
Permeate outlet temperature (°C)	24.2	24.8	25.8	26.6	27.5
Feed flow rate (l/min)			2		
Permeate flow rate (l/min)			0.2		
Feed inlet pressure (psig)			2		
Permeate inlet pressure (psig)			4		
Feed Concentration (NaCl wt.%)			3.5		
Fibers outer diameter/inner diameter/length/number			1100 μm/860 μm/16 cm/4		
Effective membrane area based on the fibers outer diameter (cm^2)	22.1				
Flux (kg/m^2hr)	14.65	22.55	38.57	54.29	70.08

instabilities such as nascent fiber collapse or deformation during the spinning of highly permeable, macrovoid-free single-layer PVDF fibers with a small wall thickness. Adopting a correct dope and coagulant chemistry can induce a big delamination between the two layers of the fibers that allows for the easy removal of the inner supporting layer after the fibers' drying stage. (2) Great flux enhancements (fluxes as high as 70 kg/m^2hr) and 100% salt rejection can be achieved in MD by optimizing the membrane morphological and geometrical properties such as porosity, pore size distribution, pores interconnectivity, and membrane wall thickness.

Acknowledgments

The authors thank Prof. J. Y. Lai at Chung Yuan Christian University and Prof. H. A. Tsai at Nan Ya Institute of Technology of Taiwan for the provision of PAN resins. The authors also thank A*Star and National University of Singapore (NUS) for funding this project with the grant number of R-279-000-218-305.

Notation

A_o = membrane total area based on the fibers outer diameter (m^2)
C_p = specific heat capacity of the permeate stream (kJ/kg ^{0}K)
J = water vapor flux (kg/m^2hr)
$\dot{m}_p$ = permeate mass flow rate (kg/hr)
N = dimensionless number
r = pore radius (m)
γ_L = liquid-vapor surface tension (J/m^2)
θ_{ef} = effective contact angle
ΔH_v = water vapor latent heat of condensation (kJ/kg)
ΔP = pressure difference at liquid-vapor interface (Pa)

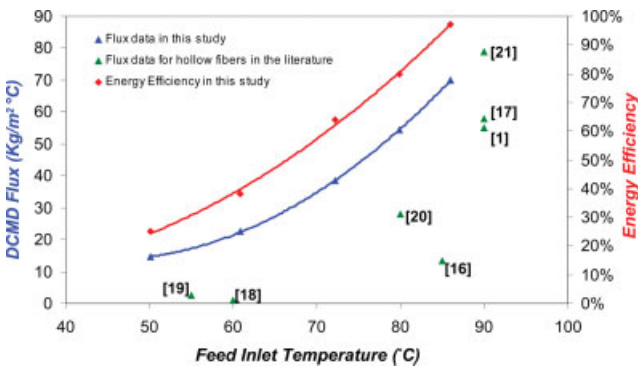

Figure 3. Flux and energy efficiency obtained in the DCMD process using the fabricated fibers and flux comparison with the literature data using hollow fiber membranes.

[Color figure can be viewed in the online issue, which is available at www.interscience.wiley.com.]

Literature Cited

1. Bonyadi S, Chung TS. Flux enhancement in membrane distillation by fabrication of dual layer hydrophilic-hydrophobic hollow fiber membranes. *J Membr Sci*. 2007;306:134–146.
2. Lawson KW, Lloyd DR. Membrane distillation (review). *J Membr Sci*. 1997;124:1–25.
3. El-Bourawi MS, Ding Z, Ma R, Khayet M. A framework for better understanding membrane distillation separation process. *J Membr Sci*. 2006;285:4–29.
4. Lawson KW, Lloyd DR. Membrane distillation. II. Direct contact membrane distillation. *J Membr Sci*. 1996;120:123–133.
5. Li Y, Chung TS. Exploration of highly sulfonated polyethersulfone (SPES) as a membrane material with the aid of dual-layer hollow fiber fabrication technology for protein separation. *J Membr Sci*. 2008;309:45–55.
6. Widjojo N, Zhang SD, Chung TS, Liu Y. Enhanced gas separation performance of dual-layer hollow fiber membranes via substructure resistance reduction using mixed matrix materials. *J Membr Sci*. 2007;306:147–158.
7. Ekiner OM, Vassilatos G. Polyaramide hollow fiber for hydrogen/methane separation-spinning and properties. *J Membr Sci*. 1990;53:259–273.
8. Wu B, Li K, Teo WK. Preparation and characterization of poly(vinylidene fluoride) hollow fiber membranes for vacuum membrane distillation. *J Appl Polym Sci*. 2007;106:1482–1495.
9. Yeow ML, Liu Y, Li K. Preparation of porous PVDF hollow fiber membrane via a phase inversion method using lithium perchlorate ($LiClO_4$) as an additive. *J Membr Sci*. 2005;258:16–22.
10. Tan X, Tan SP, Teo WK, Li K. Polyvinylidene fluoride (PVDF) hollow fibre membranes for ammonia removal from water. *J Membr Sci*. 2006;271:59–68.
11. Ren J, Wang R, Zhang HY, Li Z, Liang DT, Tay JH. Effect of PVDF dope rheology on the structure of hollow fiber membranes used for CO_2 capture. *J Membr Sci*. 2006;281:334–344.
12. Atchariyawut S, Feng C, Wang R, Jiraratananon R, Liang DT. Effect of membrane structure on mass-transfer in the membrane gas-liquid contacting process using microporous PVDF hollow fibers. *J Membr Sci*. 2006;285:272–281.
13. Wang KY, Li DF, Chung TS, Chen SB. The observation of elongation dependent macrovoid evolution in single- and dual-layer asymmetric hollow fiber membranes. *Chem Eng Sci*. 2004;59:4657–4660.
14. Li D, Wang R, Chung TS. Fabrication of lab-scale hollow fiber membrane modules with high packing density. *Sep Purif Technol*. 2004;40:15–30.

15. Li D, Chung TS, Wang R. Morphological aspects and structure control of dual-layer asymmetric hollow fiber membranes formed by a simultaneous co-extrusion approach. *J Membr Sci*. 2004;243:155–175.
16. Gryta M, Tomaszewska M, Grzechulska J, Morawski AW. Membrane distillation of NaCl solution containing natural organic matter. *J Membr Sci*. 2001;181:279–287.
17. Song L, Li B, Sirkar KK, Gilron JL. Direct contact membrane distillation-based desalination: novel membranes, devices, larger-scale studies and a model. *Ind Eng Chem Res.* 2007;46:2307–2323.
18. Li J, Xu Z, Liu Z, Yuan W, Xiang H, Wang S, Xu Y. Microporous polypropelene and polyethelene hollow fiber membranes. III. Experimental studies on membrane distillation for desalination. *Desalination*. 2003;155:153–156.
19. Fujii Y, Kigoshi S, Iwatani H, Aoyama M. Selectivity and characteristics of direct contact membrane distillation experiment. I. Permeablity and selectivity through dried hydrophobic fine porous membranes. *J Membr Sci*. 1992;72:53–72.
20. Gryta M, Tomaszewska M. Heat transport in the membrane distillation process. *J Membr Sci*. 1998;144:211–222.
21. Li B, Sirkar KK. Novel membrane and device for direct contact membrane distillation-based desalination process. *Ind Eng Chem Res*. 2004;43:5300–5309.

Manuscript received Feb. 22, 2008, revision received Jun. 2, 2008, and final revision received Sept. 11, 2008.